Controls on Development and Diversity of Early Archean Stromatolites

Controls on development and diversity of Early Archean stromatolites

*Abigail C. Allwood[1], John P. Grotzinger[2], Andrew H. Knoll[3], Ian W. Burch[4], Mark S. Anderson[1], Max L. Coleman[1], Isik Kanik[1]

[1]*Jet Propulsion Laboratory, California Institute of Technology, 4800 Oak Grove Dr, Pasadena, CA, 91109, USA*

[2]*Geological and Planetary Sciences, California Institute of Technology*

[3]*Department of Organismic and Evolutionary Biology, Harvard University, Cambridge MA 02138, USA*

[4]*Australian Centre for Astrobiology, University of New South Wales*

**Corresponding Author*: *Jet Propulsion Laboratory, MS183-301, 4800 Oak Grove Dr, Pasadena, CA, 91109, USA. Phone: +1(818) 393 4275*

Classification: Physical Sciences – geology

Number of text pages (including references and figure legends): 22

Number of figures: 6

Number of tables: 0

Supplementary information: 6 supplementary figures, 2 pages captions

ABSTRACT

The ~3450 million year old Strelley Pool Formation, Western Australia, contains a reef-like assembly of laminated sedimentary accretion structures (stromatolites) that have macroscale characteristics suggestive of biological influence (1). However, direct, microscale evidence of biology – namely, organic microbial remains or biosedimentary fabrics – has to date eluded discovery in the extensively recrystallized rocks. Recently identified outcrops with relatively good textural preservation record microscale evidence of primary sedimentary processes, including some that indicate probable microbial mat formation. Furthermore, we find relict fabrics and organic layers that co-vary with stromatolite morphology, linking morphologic diversity to changes in sedimentation, seafloor mineral precipitation and inferred microbial mat development. Thus, the most direct and compelling signatures of life in the Strelley Pool Formation are those observed at the microscopic scale. By examining spatio-temporal changes in microscale characteristics it is possible not only to recognize the presence of probable microbial mats during stromatolite development, but also to infer aspects of the biological inputs to stromatolite morphogenesis. The persistence of an inferred biological signal through changing environmental circumstances and stromatolite types indicates that benthic microbial populations adapted to shifting environmental conditions in early oceans.

INTRODUCTION

Analysis of Earth's earliest sedimentary record is crucial for understanding the early evolution of life on Earth. Stromatolites—internally laminated, macroscopic sedimentary structures, commonly of biological origin—form the dominant part of Earth's early fossil record (2) and so provide a potentially important source of information about early life. However, stromatolites are shaped by a complex interaction of physical, chemical and biological processes, and identifying unambiguous signatures of life from the preserved morphology of the structures can be extremely difficult (3-5). Ideally, textural or microstructural evidence of microbial mats is needed in addition to morphological and contextual clues in order to unravel processes of stromatolite formation and gain direct evidence of the activities of benthic microbial communities (6, 7). To date, however, the search for such clues in the oldest known stromatolites

has been frustrated by diagenetic alteration, particularly recrystallization: a diagenetic process that commonly affects the chemical (precipitated) sediments with which stromatolites are often associated.

A possible biomediated origin was previously suggested for some of Earth's oldest stromatolites, in the 3.43 Ga Strelley Pool Formation, based on their morphology (2), morphological associations and the spatio-temporal distribution of stromatolites in a reef-like palaeoenvironment (1, 8, 9). However, microfossils, microbial sedimentary fabrics and organic materials have not been identified to date. Putative microfossils and organic materials have been identified in Early Archaean rocks (10-14) but others have proposed that those are abiotic structures shaped by hydrothermal processes and composed of mantle-derived carbon (e.g. ref. 15).

Recent mapping of the Strelley Pool Formation identified several well-preserved outcrops in which relict (bio)sedimentary fabrics and carbonaceous materials could be detected and mapped within and among a variety of stromatolite forms. Here we analyze sedimentary fabrics within the context of different stromatolites and compare them with better-preserved Proterozoic examples to gain detailed, direct, microscale evidence of the physical, chemical and biological processes that contributed to stromatolite growth in the Strelley Pool Formation.

***Geologic setting**:* The Strelley Pool Formation is a ~30–400 m-thick sedimentary rock unit deposited on the Pilbara Craton between 3.43 and 3.35 billion years ago. Outcrops of the formation extend across more than 180 km (16 and references therein), but the reef-like carbonate platform buildup identified previously (1) is limited to ~10 km of outcrop in the southwestern Panorama Greenstone Belt (supporting information (SI) Fig. S1). In that area, the formation can be divided into four stratigraphic units: a basal rocky coastline conglomerate (Member 1); the stromatolitic carbonate platform member (member 2 -- further subdivided into 3 beds, each capped by a layer of large, acicular crystal pseudomorphs); a stromatolitic chert member (member 3); and a chert+volcaniclastic member (member 4). Member 2 is the focus of the present study. The principal facies of member 2 consist of: 1) six morphologically distinct types of stromatolites; 2) acicular crystal pseudomorphs that were probably originally aragonite (1); 3) flat laminites, and; 4) flat pebble intraclast conglomerates. The lithology of all member 2 facies consists of dolostone and chert (1, 8).

Sample selection and context: In the present study we examine fabrics of coniform and domical stromatolites from lower two beds of the platform carbonate (member 2). Two outcrops provide exceptional fabric preservation and exposure of those beds. The first is a ~150 meter-long section on southern "Anchor Ridge" (Fig. S1), exposing on-platform sections of bed 1 (with *encrusting/domical laminites*) and bed 2 (with three coniform stromatolite types: *cuspate swales*, *egg carton laminites* and *small conical/crested laminites*). The second outcrop is on southern "Trendall Ridge" (Fig. S1), where abundant *large complex cone* (LCC) stromatolites formed on a paleotopographic high, possibly a rimmed platform margin. The Trendall and Anchor Ridge outcrops were mapped in detail and samples were collected for slabbing, polishing and thin sectioning. Thin section microscopy and Raman spectroscopy were used to identify and analyze the fabric components, and x-ray fluorescence element imaging (acquired with a Horiba XGT-5000 X-ray analytical microscope) was used to assist in the detection of relict fabrics by mapping major and minor element distribution.

ENCRUSTING/DOMICAL STROMATOLITES

Encrusting/domical stromatolites are abundant in bed 1 of member 2 throughout the study area (1, 8). They consist of adjacent (abutting) or laterally linked pseudocolumns of domical laminae (Fig. S2). The domical laminae typically initiate on a topographic feature such as a boulder, intraclast, or small mound. In places, the domes expand radially and coalesce with each successive layer (as in Fig. S2), whereas in other places the domical laminae maintain constant dimensions through successive layers.

Here we focus on a particularly well preserved outcrop of domical stromatolites that formed on the platform interior, where bed 1 is approximately two meters thick and directly overlies altered volcanic rocks of the Mt Ada Basalt. Stromatolites initiated within 20-50 cm of the lower contact, upon surfaces defined by minor topographic irregularities associated with a flat pebble intraclast conglomerate. Several additional surfaces of stromatolite initiation occur higher in the bed. The bed thins rapidly to the north where it onlaps a paleo-high, and becomes thicker toward the south before thinning again due to underlying paleotopographic relief.

Sedimentary fabrics: Sedimentary fabrics change systematically from base to top of the stromatolite pseudocolumns. The lower parts consist of irregularly laminated dolomite and chert with discontinuous layers of carbonaceous material and chert-filled laminoid fenestrae (Fig. 1,

2e). The dolomite and chert are recrystallized, but variations in recrystallized texture hint at relict clastic and precipitated sedimentary fabrics: Although sedimentary grains are not preserved, the dolomite crystal size variations in many laminae resemble clastic sedimentary textures, and the laminae themselves have millimeter-scale irregularities and discontinuities like those associated with the trapping and binding of fine-grained particles in younger and better preserved stromatolites (17). Other laminae display faint "palisade" fabrics—consisting of sub-millimeter acicular crystals arranged perpendicular to the laminae—that indicate *in situ* precipitation and growth of crystals at the sediment-water interface (5). Chert-filled laminoid fenestrae (a type of primary or penecontemporaneous open space structure; ref. 18) are a major part of the fabric in the lower strata. The fact that they were once open spaces is indicated by the void-fill pattern of chalcedony and megaquartz within the structures (Fig. 1 b, c). Fenestrae are commonly associated with microbial mats in peritidal settings, where they often form by degassing of decaying organic material and/or drying out of the surface of microbial mats, resulting in shrinkage, lifting and separation of the mats from the sediment surface (18, p. 192-197 and references therein).

The fabric becomes more regularly laminated up section through the stromatolites, with fewer fenestrae (Fig. 2a-d) and increasing palisade fabrics. In the upper strata, the abundance of palisade fabrics and large acicular crystal pseudomorphs increases dramatically (Fig. 3 and Fig. S3c, e, f). About two meters below the upper contact of the bed, the stromatolites give way to a thick (~2 m) bed of densely-packed acicular crystal pseudomorphs (Fig. S3a,b, d).

Dolomite laminae: Under the microscope, three main types of dolomite are observed (Fig. S4). D1, the most common type, consists of roughly equigranular, anhedral crystals in a sutured mosaic—consistent with moderate to advanced dolomite recrystallization. D2 consists of very fine grained (~2 μm) dolomite, and is locally abundant around the margins of larger dolomite crystals and at the contacts between chert and dolomite laminae. D3 consists of equigranular, euhedral dolomite rhombs, or partial rhombs, with crystal growth zones (Fig. S4b). D3 crystals typically occur as overgrowths at the margins of dolomite laminae where they protrude into chert-filled fenestrae or laminae. X-ray fluorescence element maps highlight the higher iron content of D3 compared to the surrounding dolomite (Fig. 1d). The preservation of growth

zones indicate that D3 dolomite has not been overprinted by later diagenetic recrystallization, and there is no indication of major replacement of a non-carbonate phase.

Chert laminae: The chert laminae consist mainly of an equigranular mosaic of interlocking microcrystalline to mesocrystalline-quartz crystals with undulose extinction and crenulate crystal boundaries. Laminoid fenestrae in the lower parts of bed 1 have wall-coating isopachous silica cements, and radial-fibrous chalcedony, surrounding a central infilling of anhedral megaquartz (Fig. 1b,c). A few inclusions of carbonaceous material, calcite and dolomite are present.

The observed features in the chert are consistent with either: 1) selective replacement of a laminated, non-silica precursor (most likely carbonate or organic material); or 2) early diagenetic alteration of sedimentary silica laminae. It is worth noting that the observed chert fabrics do not provide unequivocal evidence that a non-silica precursor has been replaced. Early burial diagenesis of sedimentary (non-skeletal) silica involves dissolution-reprecipitation reactions that create porosity; preferentially alter some elements of the original fabric; and release SiO_4H_2 into solution, which can then re-precipitate elsewhere in the sediment pile, resulting in a mixture of original sedimentary fabrics (e.g. laminae), dissolution fabrics (cavities) and reprecipitation fabrics (cavity fill) (19). Thus, the observed diagenetic chert fabrics are not necessarily evidence of replacement of a non-silica precursor. Moreover, the chert laminae are present in intraclast conglomerate clasts within beds 1, 2 and 3—this supports a primary or very early diagenetic origin and is not consistent with a late stage (post-member 2 deposition) hydrothermal replacement origin as proposed previously (20).

Organic laminae*:* Raman spectra confirm that black laminae within the stromatolite fabric consist of disordered carbonaceous material (Fig. S5). The spectral characteristics of the organic matter are similar to those exhibited by the Strelley Pool Formation samples examined previously and are consistent with the regional lower greenschist metamorphism (21). This indicates that the organic material has been subject to the thermal history of the host rock and did not migrate recently into the bed. Significantly, the organic laminae are also preserved in flat pebble intraclast conglomerates that onlap the stromatolites (Fig. 1a, e, f). The organic matter is concentrated in a discrete layer on the upper side of the intraclasts, and is partially intermingled with the dolomite (D1/D2) that makes up the clasts. Furthermore, the organic layer was then overgrown by D3 dolomite crystals that surround the clasts. The clasts, organics and D2

dolomite overgrowths are then surrounded by isopachous chert rims and chert matrix, both of which contain no organic matter. Thus, it seems very unlikely that the organic matter migrated through the matrix and coated the clasts after burial. The weight of evidence indicates that the organic layers were synsedimentary laminae formed at the stromatolite-water interface during deposition, and are not younger contaminants introduced to the rock during diagenesis.

Having determined with reasonable certainty that the organic laminae in the encrusting/domical stromatolites are syngenetic, multiple hypotheses for the origin of the organic material remain to be tested. On the one hand, the laminae could represent allochthonous organic detritus transported and settled onto the stromatolites, in which case either biotic or abiotic (mantle or meteorite-derived) ultimate origins are possible. Alternatively, the organic laminae could be the remains of microbial mats formed *in situ* at the sediment-water interface.

Under transmitted light, the organic laminae are seen to consist of sub-millimeter-sized amorphous clots, specks and wisps of opaque material included in crystals or accumulated along dolomite grain boundaries, where it appears to have been displaced by the margins of growing crystals during recrystallization. Insufficient morphological detail has been preserved to determine whether microbial cells were once present as part of a microbial mat. Biogenic and abiogenic hypotheses must therefore be tested using attributes at scales large enough to survive recrystallization. At the naked eye and hand-lens scale, the polished slabs display sufficient attributes to test those hypotheses.

A hypothesis that proposes the laminae are formed of allochthonous organic detritus would predict that the organic particles were subject to current reworking and gravity-driven settling, and therefore tend to accumulate in lows. They would also potentially mix with other grain types. Such fabrics are not observed. Rather, the stromatolites have discrete, organic-rich, wrinkly laminae between sediment layers, indicating distinct episodes of organic layer formation (Fig. 1a, 2). Moreover, the organics formed mat-like layers that contoured the stromatolites from cusp to cusp; did not thicken into lows; and possessed sufficient cohesive / adhesive properties to enable their establishment on stromatolite margin slopes greater than the angle of repose for particulate sediment (around 30^{o} (22)) (Fig. 1a, 2a, b, f). Thus, the organic layers likely do not consist of transported allochthonous organic detritus. Rather, their character and distribution are

consistent with their interpretation as the remains of microbial mats formed at the sediment-water interface—in many places on steep to near-vertical slopes—during stromatolite growth.

This leads to the question of the role of microbes in stromatolite accretion, which requires an understanding of the roles of *in situ* chemical precipitation (i.e. precipitation at the sediment-water interface) and "clastic" sedimentation (i.e. mechanical deposition of sediment particles, including mineral particles formed by precipitation in the water column). In the case of clastic sedimentation, active microbial trapping and binding would be the only plausible way to accumulate sediment on steep- to vertical-sided domes. In the case of *in situ* precipitation, sediment can accumulate on any slope with or without the presence of microbial mat. However, in a precipitative environment microbes could also have played two roles influencing the precipitation of sediment: metabolically inducing mineral precipitation within the mat microenvironment, or forming an organic "template" for localization of mineral precipitation.

Determining the nature of the primary sediments (precipitated in situ vs. clastic) is hampered by the absence of pristine primary fabrics or interspace deposits between stromatolites—which might have offered clues in sedimentary fabrics not modified by stromatolite-forming processes. However, valuable insights are nonetheless recorded within the stromatolites themselves: in the relict fabrics and geometry of the laminae, and their co-variation through time. Many stromatolite laminae retain faint vestiges of clastic or palisades/crystal fabrics. Laminae with probable clastic character are more prevalent in the lower strata (Fig. 1, 2) whereas precipitated (palisades) fabrics become more abundant in the upper strata (Fig. 3b, c, and Fig. S3). This vertical transition is matched by a change in lamina geometry: most of the laminae in the lower strata become thinner toward the stromatolite margins (Fig. 2a, b), as would be expected if microbes were actively trapping and binding sediment or causing intra-mat precipitation—leading to thicker accretion on horizontal surfaces. Laminae in the upper strata, on the other hand, are isopachous, as expected if the layers formed dominantly by surface-normal crystal growth (5). These parallel changes in fabric and morphology suggest that stromatolite accretion was initially dominated by microbial trapping and binding of sediment and/or intra-mat precipitation, but became increasingly dominated by *in situ* precipitation through time. Importantly, the stacking of marginal-thinning laminae in the lower strata resulted in minimal change in laminae morphology during early stromatolite growth, whereas stacking of isopachous, precipitated laminae during later growth resulted in cusp infill and coalescence of

the domes (Fig. 3). The correlation between changes in stromatolite morphology and sedimentary process, as inferred from fabrics and laminar architecture, conforms well to expectations from theoretical models of stromatolite morphogenesis (5, 23, 24) for a system evolving from microbially dominated to precipitation-dominated accretion. Therefore it is reasonable to conclude that benthic microbial communities or colonies contributed to formation of the encrusting/domical stromatolites, but their morphogenetic influence decreased over time as chemical precipitation increased.

CONIFORM STROMATOLITES

The coniform stromatolites of member 2/bed 2 contrast markedly to the encrusting/domical stromatolites of bed 1 in terms of fabrics as well as morphology. Here we examine two types of coniform stromatolites to analyze these differences: the "large complex cone (LCC) stromatolites," which occur mainly near the platform margin, and the pseudo-conical "cuspate swale stromatolites," which dominate the platform interior.

Well preserved LCC specimens were collected from an outcrop on southern "Trendall Ridge", where abundant stromatolites clustered on the high side of a rim-like topographic feature at the platform margin (Fig. 4). Cuspate swale stromatolite samples were collected at southern "Anchor Ridge." Both stromatolite types consist of alternating dolomite and chert laminae. The LCC structures have distinctive coniform morphology (Fig. 4) that is inherited through stacks of laminae that form pseudocolumns up to 2 meters high (i.e. 2 meters stratigraphic thickness) (1). Individual stromatolites are laterally separated by a few centimeters up to several decimeters of flat-lying laminated dolomite-chert. The cuspate swale stromatolites consist of pseudo-conical structures with concave-upward slopes that grade into trough-shaped interspaces (Fig. S6). The apices of adjacent structures are connected by saddle-shaped ridges) (1).

One notable aspect of the fabrics in both LCC and cuspate swale stromatolites is the high degree of lateral correlation between stromatolite and intercolumn laminae, which attests to uniform rates of accumulation and *some commonality* of depositional process between stromatolite and intercolumn areas. However, another notable feature is the contrast between the type of fabrics seen in the stromatolite and intercolumn areas (Fig. 5a), which attests to differences in the processes occurring in the two areas.

The intercolumn fabric is characterized by slightly to moderately undulose laminae that thicken and thin laterally. Current scours, topographic infill geometry (e.g., onlap, drape), tangential truncations, low-angle cross laminations and graded fabrics are well-expressed and abundant (Fig. 5a). Together, these features indicate deposition of clastic sediment from current and wave-agitated water. However, rather than being defined by changes in size and composition of clastic grains (none are visible due to recrystallization), they are defined by variations in size and type (i.e. chert, D1, D2 or D3 dolomite) of the neomorphic crystals. Here we infer that crystal size, in a relative sense, approximates sediment grain size—although this cannot be demonstrated due to the complete absence of primary grains, the distinct relationship of crystal size to stratification style supports this inference. In contrast to the intercolumn fabrics, the stromatolite interior fabrics consist of thin, continuous, nearly isopachous laminae reminiscent of precipitated layers. In the case of the cuspate swales there is a gradual lateral transition between the two fabrics across the concave slope (Fig. S6), whereas in the LCC stromatolites the transition is very sharp across an abrupt slope change. This contrast between stromatolite and intercolumn fabrics persists through many hundreds of laminae, attesting to long-lived differentiation of sedimentary processes on the stromatolites compared to the intercolumn area.

Although presence of a benthic microbial community could cause such highly localized and sustained modification of sedimentary process, the textural hallmarks typically associated with microbial mat buildup are absent: namely, wrinkled or crinkly laminoid fabrics, fenestrae and organic laminae (organic matter is rare, occurring only as faint, lamina-parallel wisps of organic material in some samples). However, it is also true that neither precipitation nor clastic sedimentation alone satisfactorily explains the combination of stromatolite and intercolumn area fabrics. It also seems unlikely that *in situ* precipitation on the stromatolite was juxtaposed against clastic sedimentation in the intercolumn areas, because—as already noted—the lateral correlation of intercolumn and stromatolite laminae indicates that material both on and off the stromatolites accumulated at a uniform rate, signifying commonality of depositional process.

An alternative hypothesis that incorporates *alternating* clastic sedimentation and biofilm-nucleated precipitation arises from comparison with Mesoproterozoic *Omachtenia omachtensis* and *Gongylina differenciata* stromatolites (Uchuro-Maya region, Siberia) (25). The microstructure of those stromatolites formed by emplacement of mm-scale sediment-rich laminae during depositional events such as storms or high tides, alternating with development of

thin, laterally continuous micritic laminae, preserved by penecontemporaneous mineral precipitation within thin organic sheets (Fig. 5b). Silicified structures show that the organic sheets formed through decay of microbial mats that inhabited and stabilized the sediment surface during intervals of non-deposition (25).

In the Strelley Pool Formation, the thin, near-isopachous laminae that span the coniform stromatolites and the intercolumn areas (e.g. location 1, Fig. 5a) resemble *Omachtenia's* organic-sheet-nucleated precipitates, while the undulating intercolumn deposits resemble the "sedimentary event beds". Thus, the processes inferred for formation of *Omachtenia* and *Gongylina* stromatolites may also explain coniform stromatolite development in the Strelley Pool Formation (Fig. 6). However, closer examination of LCC and cuspate swale stromatolites suggests some minor differences.

The *Omachtenia* style of stromatolite morphogenesis involves temporal (rather than spatial) variations in sedimentary regime, and implies that contemporaneous sedimentary layers should therefore exhibit the same fabric, having formed under the same regime. In the LCC stromatolites this is true at some stratigraphic levels—some stromatolite laminae correlate with similarly thin, isopachous laminae in the intercolumn area, while clastic deposits lie above and below those, reflecting temporal alternation between two regimes. However, there are many places (e.g. location 2 and 3, Fig. 5a) where sets of stromatolite laminae (with precipitate-like fabric) transit directly across the stromatolite margins into a set of correlative—and therefore contemporaneous—"clastic" laminae. Evidently, there were spatial variations in the way those laminae formed.

These relationships indicate that at least some organic films influencing formation of laminae on the stromatolite terminated at the stromatolite margins. In addition, the direct correlation of stromatolite laminae with clastic intercolumn deposits may indicate that the stromatolite laminae formed by microbial adhesion of clastic sediment, rather than by *in situ* precipitation on the organic films. We have argued against microbial trapping and binding of sediment particles on the stromatolite due to the lack of textural evidence in the stromatolitic laminae. However, a possible explanation for this apparent paradox involves settling of micrometer-scale, water column-nucleated crystals onto both the stromatolite (whereupon they adhered to an organic layer) and the intercolumn surfaces (where no organic layer existed and the particles could be

moved around by currents and waves), thereby creating a single layer with lateral variation in cohesiveness. Deposition of water column-nucleated precipitates is a well documented phenomenon in precipitative environments such as evaporite basins (26 and references therein). Such extremely fine crystals settling from the water column may not require a well-developed, trapping and binding mat community in order to adhere to stromatolite slopes. A thin organic film could have sufficed —either a thin biofilm, or decayed mat remnants like those observed in *Omachtenia* and *Gongylina*, and inferred here to have been templates for precipitation. Experiments have shown that the presence of a thin, low profile but mucilaginous organic film on a submerged surface greatly enhances sediment particle adhesion, even under flow conditions (27). Thus, the presence of a either a low profile biofilm or the decayed remnants of a mat on the stromatolite could have facilitated particle adhesion.

The surviving textural evidence cannot be used to discriminate between this latter hypothesis and the hypothesis that the stromatolite laminae formed by localized in situ precipitation. Potentially, a combination of grain adhesion and mat-nucleated precipitation could have contributed to stromatolite accretion. However, the "grain adhesion" hypothesis better explains the consistent vertical thickness of laminae throughout stromatolite and intercolumn areas, and resulting consistency of laminar geometry through the pseudocolumn (1). Such geometry is consistent with vertical settling of particles onto the surface.

In summary, formation of Strelley Pool Formation coniform stromatolites likely involved a combination of the following "sedimentation/accretion modes" (illustrated in Fig. 5a and 6):

1. formation of laterally extensive laminae by precipitation within thin organic layers (location 1, Fig. 5a)
2. rare deposition of laterally restricted sedimentary "event" layers in the low areas between stromatolites (location 4, Fig. 5a)
3. Formation of laterally variable laminae from accumulation of "clastic" layers between stromatolites (consisting of water-column precipitated particles) coupled with either: (a) adhesion of water column-nucleated particles to thin organic films on stromatolites; or (b) localized precipitation of laminae on stromatolites, nucleated on thin organic layers. (location 2 and 3; Fig. 5a)

In reality there were probably infinitely variable intermediate modes, combining aspects of these three “end member” modes. However, there also appear to be relatively distinct examples of the fabrics associated with each end member mode. The changing relative importance of each of these modes of accretion/deposition through time can be traced through the changing arrangement of the different fabric suites.

In this view, the role of microbes in coniform stromatolite accretion was largely passive. Microbes simply provided a layer of organic material that formed a template for crystal nucleation and/or particle adhesion. Accepting this, the most direct evidence for microbial involvement in stromatolite morphogenesis comes from not stromatolite morphology, or from specific textural observations in isolation, but from the spatio-temporal arrangement of textures and fabrics within the context of stromatolite morphology. If morphology does not of itself encapsulate the microbial influence, then it is unlikely that a morphotype can be definitively linked to a specific type of organism, or even a metabolic strategy such as photosynthesis (28).

GENESIS AND VARIABILITY OF STROMATOLITES

The existence of microbial mats during formation of stromatolites in the Strelley Pool Formation can be deduced from different sets of evidence in multiple stromatolite types. In domical stromatolites, evidence of microbial mat formation lies in the observation that cohesive layers of organic material formed at discrete, regular intervals at the surface of stromatolites, coupled with the fact that those laminae adhered to the steep stromatolite margins and did not preferentially thicken into topographic lows. In the coniform stromatolites, microbial activity is inferred from the juxtaposition of contemporaneous but contrasting sedimentary fabrics and their arrangement within the context of stromatolite morphology. In both instances the interpretation benefits from comparisons with microbially-influenced microstructure in well-preserved Proterozoic stromatolites (24). Unfortunately, microfossils are not preserved due to redistribution of the organic material by neomorphic crystal growth during recrystallization. Biomarker preservation is possible but perhaps unlikely due to the thermal maturity of the organic matter (29).

In addition to preserving different types of biosignatures, the stromatolites also preserve evidence that microbes played a variable role in accretion. In coniform stromatolites, microbes may simply have provided a template—perhaps *post-mortem*—for chemical precipitation or adhesion of fine crystalline sediment nucleated in the water column. In the encrusting/domical

stromatolites, thinning of laminae at the margins suggests a component of active microbial trapping and binding, and/or intra-mat biomediated precipitation, which gave way through time to *in situ* precipitation during later stages of accretion. Effectively, the proportion of microbial mat formation—relative to other processes of deposition—played a role in determining stromatolite morphogenetic variability.

Whether biological factors were the principal control on stromatolite *initiation* is unclear from either fabrics or morphology. However, some contextual features provide insight to alternate possibilities. A major clue is the fact that most stromatolites appear to initiate on a pre-existing topographic feature such as an intraclast, cobble, boulder, ripple crest or mound. Microbial colonization and biofilm formation at the benthic boundary layer can hinge upon subtle lateral topographic variations that affect fluid circulation and chemical gradients in pore spaces of the upper millimeters of sediment (30). Thus, slightly elevated locations such as ripple crests are differentiated from their surroundings—from an ecological or biochemical point of view—in terms of pore space chemistry, and could become preferred substrates for local mat formation and stromatolite initiation. Precipitation could also occur preferentially on highs, as elevated sites would be more likely to remain free of sediment, enabling uninterrupted crystal growth. However, evidence from Proterozoic rocks suggests that seafloor carbonate precipitation can be facilitated by or nucleated within mats (e.g.14)—a process that is also inferred here for "established" stromatolites in the Strelley Pool Formation. Thus if the better-understood, younger geologic record is the key to the deep past, then microbial colonization and biofilm formation may have been the initializing factor, leading to subsequent mat-nucleated precipitation or particle adhesion. Experimental work may determine whether this latter hypothesis is likely, or whether seafloor precipitation could equally have provided rapid initial stabilization of the sediment, prior to microbial colonization on the highs.

While the location and relative amount of microbial mat formation played a role in determining stromatolite initiation, distribution and morphogenesis, this does not necessarily imply that stromatolite morphologic changes equate to biodiversity. Changes in stromatolite morphology described herein are evidently linked to shifts in environmental processes through the Strelley Pool Formation. For example, in the case of domical stromatolites, the change from inherited to coalescing morphology through time is clearly linked to increasing precipitation, as evidenced in the vertical increase in crystals and palisades fabrics (Fig. 3). Furthermore, the change from

domical to coniform morphology is accompanied by a relative decrease in evidence for precipitation. These latter observations conform well to model predictions of shifting interaction between the amount of surface-normal growth driven by *in situ* precipitation and the amount of vertical growth driven by microbial processes (23). There is no biodiversity implicit in this relationship; simply a change in the relative influence of microbial input compared to other processes. The textural and morphological evidence described herein do not provide direct evidence of biodiversity, and without microfossils it is impossible to test the null hypothesis that the entire stromatolite assemblage involved just one type of microorganism. Nonetheless, the environmental changes that accompanied stromatolite morphologic changes imply that microbial communities at the stromatolite surfaces had to 'adapt' to those changes.

It is clear from sedimentological evidence that any microbial communities present during deposition of the Strelley Pool Formation would have been subject to significant environmental shifts, including changes in water depth, sedimentation rate, precipitation rate and wave or current energy. Extant microbial systems respond to such changes by altering the survival strategies or gene expression of individual species, as well as the composition of multi-species communities. Therefore, to the extent that modern analogs guide interpretation of ancient processes, then ecologically diverse microbial mat communities were probably involved in stromatolite formation, and changed their community composition and survival strategies in response to changing environmental conditions. Those changes may be reflected in the diverse array of stromatolite morphologies and textures that formed during deposition of the Strelley Pool Formation.

One important question involves the possible role of photosynthetic organisms in early Archean mat communities (e.g. 31). Early studies of modern tufted mat stromatolites suggested coniform morphology was caused by the phototactic aggregation of filamentous cyanobacteria (32). However, recent experimental results on tuft formation under variable illumination conditions indicate that coniform morphology can develop independently of photosynthesis (28). The morphology of Strelley Pool Formation coniform stromatolites suggests a tendency for vertical growth (1), which has been attributed to the vertical migration of photosynthetic microbial communities (23). However, chemotaxis and the settling of sediment could— in principal—play the same role in causing vertical growth in stromatolites. That is, continuing sediment deposition could prompt migration of microbes toward the sediment-water interface, along a vertical

chemical gradient in the upper millimeters of sediment. Thus, whether or not photoautotrophs were included within Strelley Pool Formation microbial communities is unclear from either textural or morphological evidence. Perhaps the best evidence for possible photoautotrophs in former Strelley Pool microbial communities lies in the effect of water depth, and inferred seafloor illumination, on stromatolite distribution. Previous studies documented a regional trend wherein stromatolites occur only in the shallow water parts of the Strelley Pool Formation carbonate platform, and are absent in laterally equivalent deeper water deposits. The present study documents even more compelling evidence for this relationship along southern "Trendall Ridge", where stromatolite distribution across relict topography at the platform margin was very tightly controlled by water depth. (Fig. 4a).

In conclusion, evidence preserved in the Strelley Pool Formation suggests that microbial mat communities probably existed 3.43 billion years ago in the Pilbara sea, flourishing under shifting environmental conditions, resulting in a morphologically diverse assemblage of stromatolites. These stromatolites may have been inhabited by diverse microbial communities, possibly including photoautotrophs.

ACKNOWLEDGEMENTS

We are deeply grateful to the Geological Survey of Western Australia for generous field support. We also express our gratitude to Malcolm Walter and Arthur Hickman for helpful discussions, and to Dawn Sumner and Ian Fairchild for comprehensive and helpful reviews. Travel costs were partly supported by the Agouron Institute. Allwood is supported by the NASA Postdoctoral Program.

REFERENCES

1. Allwood AC, Walter MR, Kamber BS, Burch IW (2006). Stromatolite reef from the Early Archaean era of Australia. *Nature* 414:714-718.

2. Hofmann H (2000) in *Microbial Sediments,* eds Riding R, Awramik S (Springer-Verlag, Berlin, Heidelberg) pp 315-327.

3. Semikhatov M, Gebelein C, Cloud P, Awramik S, Benmore W (1979) Stromatolite morphogenesis—progress and problems. *Can. J. Earth. Sci.* 19:992–1015

4. Grotzinger J, Rothman D (1996) An abiotic model for stromatolite morphogenesis. *Nature* 383:423-425.

5. Grotzinger J, Knoll A (1999) Stromatolites in Precambrian carbonates; evolutionary mileposts or environmental dipsticks*? Annu. Rev. Earth. Planet. Sci.* 27:313-358.

6. Buick R, Dunlop J, Groves D (1981) Stromatolite recognition in ancient rocks: An appraisal of irregularly laminated structures in an Early Archaean chert-barite unit from North Pole, Western Australia. *Alcheringa* 5:161-181.

7. Awramik SM, Grey K (2005) Stromatolites: Biogenicity, biosignatures, and bioconfusion. *Proc. SPIE* 5906 1-9

8. Allwood A, Walter M, Burch I (2007) Stratigraphy and Facies of the 3.43 Ga Strelley Pool Chert in the Southwest North Pole Dome. *Western Australia Geological Survey Record* 2007/11. 28pp.

9. Allwood A, Walter M, Burch I, Kamber B (2007) 3.43 billion-year-old stromatolite reef from the Pilbara Craton of Western Australia: Ecosystem-scale insights to early life on Earth. *Precamb. Res.* 158:198-227.

10. Awramik S, Schopf J, Walter M, Weber R, Guerrero J (1983) Filamentous fossil bacteria from the Archaean of Western Australia. *Precamb. Res.* 20:357-374.

11. Schopf J, Packer B (1987) Early Archaean (3.3-billion to 3.5-billion-year-old) microfossils from Warrawoona Group, Australia. *Science* 237:70-73.

12. Schopf J (1993) Microfossils of the early Archaean Apex Chert; new evidence of the antiquity of life. *Science* 260:640-646.

13. Ueno Y, Isozaki Y, Yurimoto H, Maruyama S (2001) Carbon isotopic signatures of individual Archean microfossils (?) from Western Australia. *Int. Geol. Rev.* 43:196–212.

14. Westall F, de Vries, S, Nijman W, Rouchon V, Orberger B, Pearson V, Watson J, Verchovsky A, Wright I, Rouzaud J-N, Marchesini D, Anne S (2006) in *Processes on the Early Earth*, eds Reimold WU and Gibson R (Geological Society of America Special Publication) pp 105-131.

15. Brasier M, Green O, Jephcoat A, Kleppe A, Van Kranendonk M, Lindsay J, Steele A, Grassineau N (2002) Questioning the evidence for Earth's oldest fossils. *Nature* 416:76-81.

16. Hickman, A.H., 2008. Regional review of the 34236-3350 Ma Strelley Pool Formation, Pilbara Craton, Western Australia. *Western Australia Geological Survey Record* 2008/15.

17. Walter MR (ed), (1976) Stromatolites (Elsevier, Amsterdam). 790pp.

18. Flugel E. Microfacies of Carbonate Rocks (Springer, Berlin, 2004). 976pp.

19. Jones B, Renaut R (2007) Microstructural changes accompanying the opal-A to opal-CT transition: new evidence from the siliceous sinters of Geysir, Haukadalur, Iceland *Sedimentology* 54, 921-948.

20. Van Kranendonk MJ, Pirajno F (2004) Geochemistry of metabasalts and hydrothermal alteration zones associated with c. 3.45 Ga chert and barite deposits: implications for the geological setting of the Warrawoona Group, Pilbara Craton, Australia. *Geochem. Explor. Environ. Anal.* 4:253-278.

21. Allwood AC, Walter MR, Marshall CP (2006b). Raman spectroscopy reveals thermal palaeoenvironments of c.3.5 billion-year-old organic matter. *J. Vib. Spec.* 41:190-197

22. Bagnold RA (1956) The flow of cohesionless grains in fluids. *Royal Soc. London Philos. Trans. Ser. A* 249 235-297

23. Batchelor M, Burne R, Henry B, Slatyer T (2005) Statistical physics and stromatolite growth: new perspectives on an ancient dilemma. *Physica A* 350:6-11

24. Dupraz C, Pattisina R, Verrecchia E (2006) Translation of energy into morphology: Simulation of stromatolite morphospace using a stochastic model. *Sediment. Geol.* 185: 185-203.

25. Knoll A, Semikhatov M (1998) The genesis and time distribution of two distinctive Proterozoic stromatolite microstructures. *Palaios* 13;408-422.

26. Warren J (1999) Evaporites. Their Evolution and Economics. (Blackwell Science, Oxford), 438pp.

27. Salant NL, Hassan MA (2007) "Sticky Business": The influence of surface biofilm on particle deposition and infiltration in streams. *American Geophysical Union, Fall Meeting*, abstract #H13D-1534

28. Shepard R, Stork N, Oberstadt A, Armstrong D, Sumner D (2008) Random motility creates reticulate morphologies in cyanobacterial biofilms, leaving phototaxis in the dark. *Astrobiology* 8: Abstract 18-15-O

29. Summons R, Albrecht P, McDonald G, Moldowan J-M (2008) Molecular Biosignatures *Space Sci. Rev*. 135: 133-159

30. Fenchel T (2002) Microbial behavior in a heterogeneous world. *Science* 296:1068-1071

31. Tice MD, Lowe DR (2004) Photosynthetic microbial mats in the 3416-Myr-old ocean. *Nature* 431:549–552.

32. Walter MR, Bauld J, Brock TD (1976) in *Stromatolites*, ed Walter MR. (Elsevier Science, Amsterdam) pp 273–-310.

FIGURE CAPTIONS

Figure 1: Encrusting/domical stromatolite fabrics. (a) Polished slab, showing irregular wrinkly laminar fabric consisting of dolomite (D), chert (C) and organic laminae (OM). Note organic layers on upper sides of flat pebble intraclast conglomerate (Cg – outlined in dotted red line) piled against upper right of stromatolite. (b) Photomicrograph of chert filled fenestral void surrounded by D2 dolomite. Transmitted plane polarized light. (c) Photomicrograph showing detail of cavity fill chert with chalcedony at margins and megaquartz at the centre. Transmitted cross polarized light. (d) Composite X-ray fluorescence (XGT) map of Ca (blue) and Fe (pink). The brighter pink areas highlight the greater Fe content of D3 dolomite compared to D1 and D2 in the surrounding dolomite (blue) laminae. The black areas in the rock fabric represent silica. Scale bar in d = 1 cm. (e) Detail if intraclast conglomerate from upper right corner of sample shown in (a). Red arrows point to white rims surrounding the clasts and organic material. The rims consist of D2 dolomite overgrowths (inner) and isopachous chert rims (outer). (e) Schematic illustration of the relationship between clasts, organic deposits, dolomite overgrowths and chert in the intraclast conglomerate shown in (d).

Figure 2: Fabrics in lower to middle strata of encrusting/domical stromatolites at "Anchor Ridge". (a) Polished slab showing edge of domical stromatolite with organic laminae and variable recrystallization. Note laminae become thinner toward margin, as shown by the dotted white lines and large arrows oriented normal to the paleosurface of the stromatolite. As a result, the cusp and dome geometry do not change significantly through successive layers. g = inferred clastic or 'grainy' fabric; p = relict palisades (precipitated) fabric; o = organic laminae. (b) Polished slab showing edge of domical stromatolite with organic laminae and variable recrystallization. Note laminae become thinner toward margin, as shown by the dotted white lines. (c) Polished slab showing detail of inferred relict clastic texture with organic laminae (black layers) and dolomite laminae with minor chert (grey layers). (d) Polished slab showing detail of inferred clastic texture with organic laminae (black layers) and incipient domical structures. (e) Polished slab showing detail of irregular laminoid fabric with organic laminae, chert-filled fenestrae and relict grainy texture. Scale bar in all images is approximately 1cm.

Figure 3: Images showing the vertical trend in fabrics and parallel change in laminar architecture through the encrusting/domical stromatolites. (a) Outcrop exposure showing part of two broad domical stromatolites and the cuspate depression in between. The lower strata show irregularly laminated fabrics with inferred clastic textures; laminae thin toward the margins and laminar geometry does not change significantly through successive layers. The abundance of precipitated textures (palisades, acicular crystal psedudomorphs) increases in the upper strata, where laminae maintain thickness laterally and the laminar geometry changes with each successive layer. Consequently, the cusp infills and the domes coalesce. Scale increments on card = 1cm. (b) Polished slab showing acicular crystal pseudomorphs from strata approximately 30 cm above the top of the photo in (a). (c) Polished slab showing palisaded layer amongst irregular lamination. (d) Polished slab showing irregular lamination with organic layers (black laminae).

Figure 4: Stromatolites at the platform margin - outcrop on southern "Trendall Ridge". (a) Outcrop map showing cross-section view of stratigraphy from underlying altered volcanic rocks up through Members 1, 2, 3 and part of Member 4 of the Strelley Pool Formation. Note the paleotopographic feature on which the stromatolites were deposited: stromatolites only formed on the high side (right). Letters denote location of remaining figures. (b) Wavy laminites deposited in deeper water south of the paleohigh. (c) LCC (conical) stromatolites formed on the paleohigh. The dotted white line traces a single lamina across two coniform stromatolites. The sample indicated is shown in Figures 10 and 13b. (d) Interbedded flat laminites and lenses of crystal pseudomorphs and local erosion surfaces overlying the stromatolites in bed 2 on the paleohigh. (e) Detail of conical stromatolite margin showing onlapping undulose laminated sediments (right) and evenly laminated conical stromatolite fabric (left).Scale rule in b, c, d = 15cm. Increments on rule in e = 1cm. Modified from/Published with permission…(awaiting advice on whether copyright permission is required).

Figure 5: Sedimentary fabrics of an Early Archean coniform stromatolite and Mesoproterozoic *Omachtenia* stromatolite. (a) Coniform "large complex cone" stromatolite from the Early Archean Strelley Pool Formation stromatolite – the stromatolite is on the right and flat-lying intercolumn laminae are on the left. Polished slab, cross section view. Dark laminae are chert-rich, light laminae are dolomite-rich. Dark cross cutting fractures filled with hematite are the

result of recent weathering. Dotted white lines highlight bundles of laminae with different character. Numbers refer to explanation in text. (b) *O. omachtensis* stromatolite from the Uchuro-Maya region, Siberia, showing precipitated and clastic textures with thin organic laminae. Thin section, plane polarized light. Colored arrows on laminae in (a) and (b) indicate the different processes those laminae are inferred to have formed by. See legend at base of figure for explanation of colors.

Figure 6: A simplified schematic representation of two inferred modes of formation of coniform stromatolites in the Strelley Pool Formation - incorporating spatial and temporal variations in process sequences – and the resulting sedimentary fabrics in relation to morphology. The first mode (left side) is similar to the sequence of processes that formed Proterozoic *Omachtenia* stromatolites, and involves temporal variations in laterally uniform processes [24]. The second mode (right side) also involves lateral variations in process due to the formation of microbial films only on stromatolites

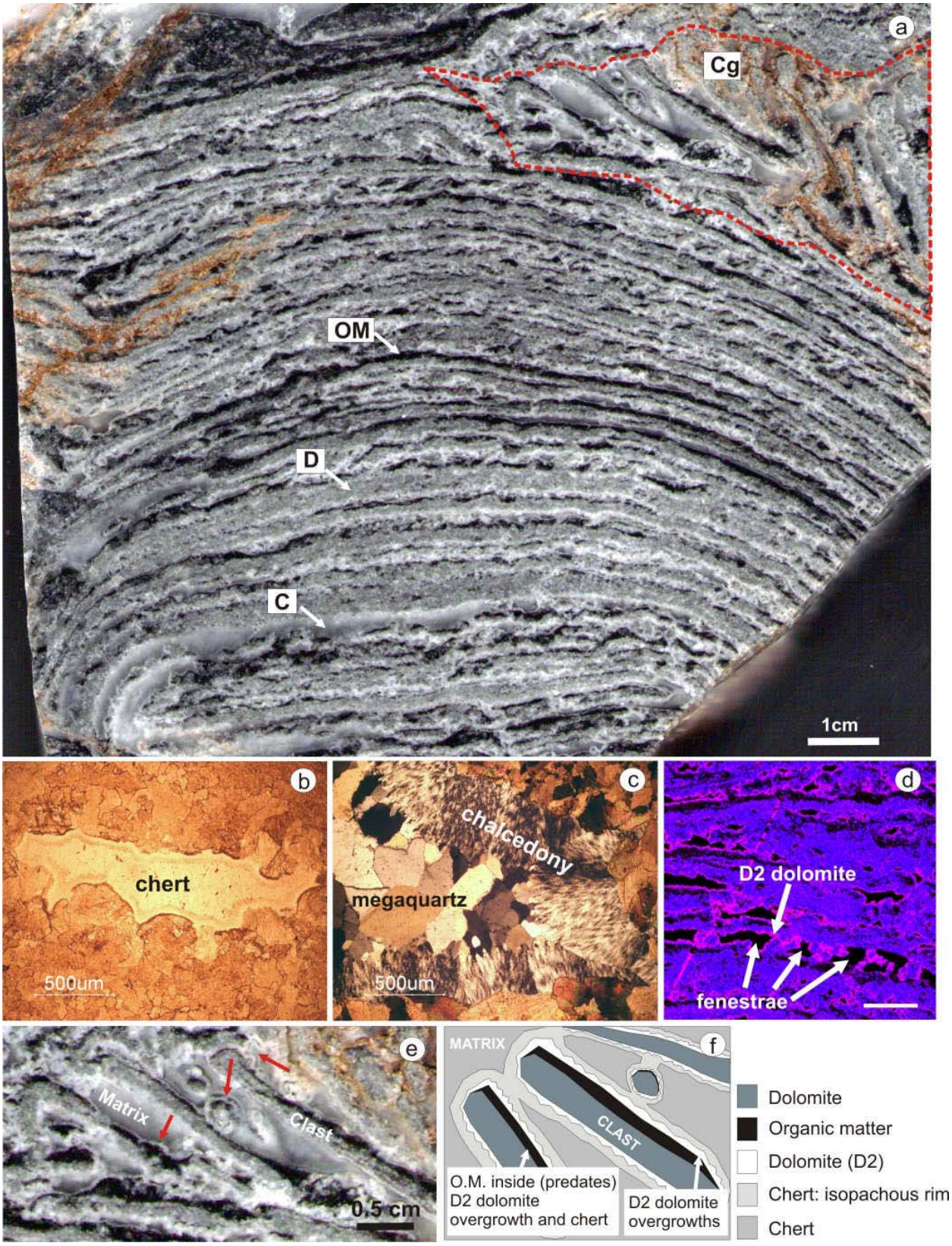
a
Cg
OM
D
C
1cm
b
chert
500um
c
chalcedony
megaquartz
500um
d
D2 dolomite
fenestrae
e
Matrix
Clast
0.5 cm
f
MATRIX
CLAST
O.M. inside (predates) D2 dolomite overgrowth and chert
D2 dolomite overgrowths
Dolomite
Organic matter
Dolomite (D2)
Chert: isopachous rim
Chert

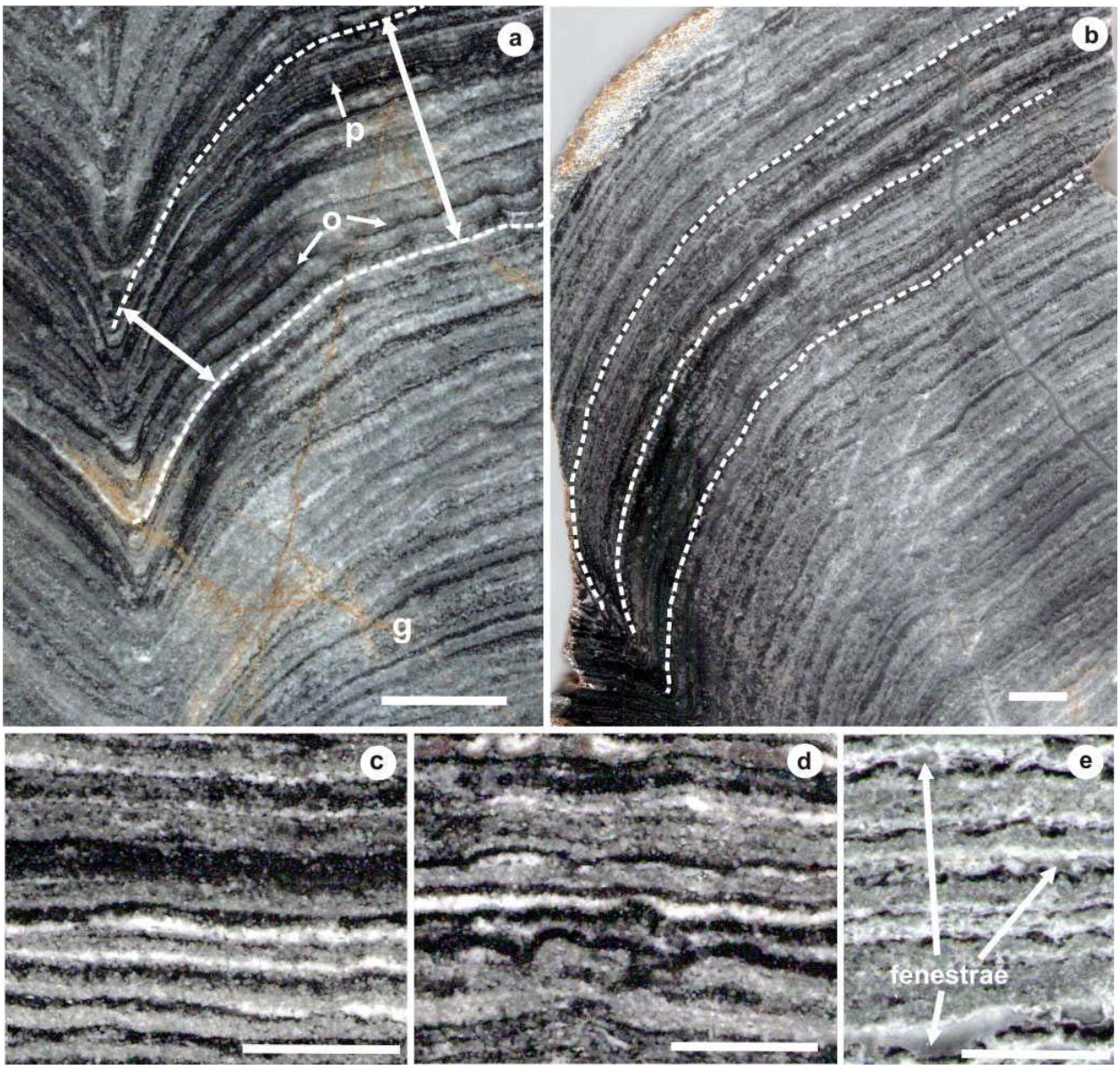
a
p
o
g
b
c
d
e
fenestrae

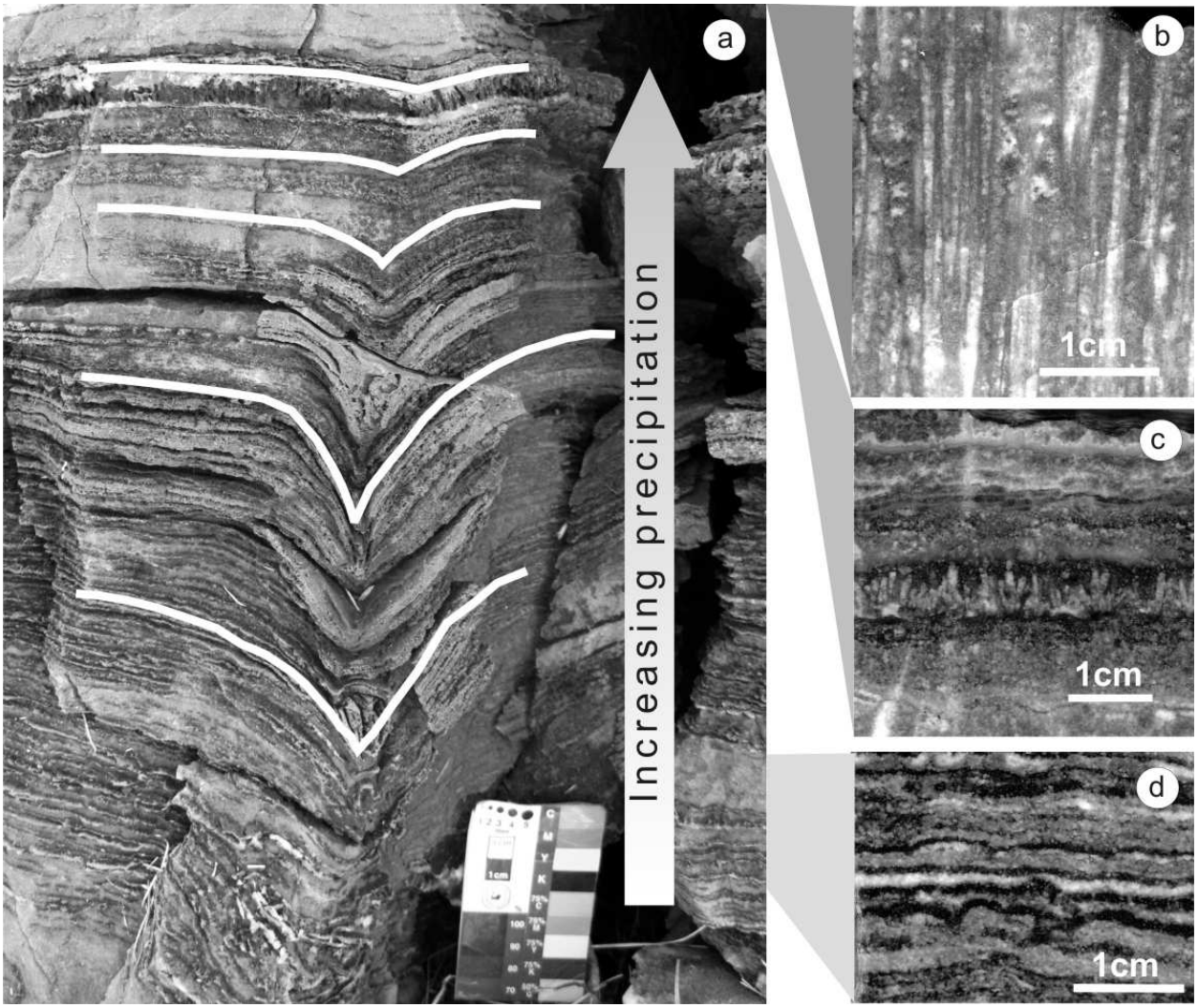
a
Increasing precipitation
b
1cm
c
1cm
d
1cm

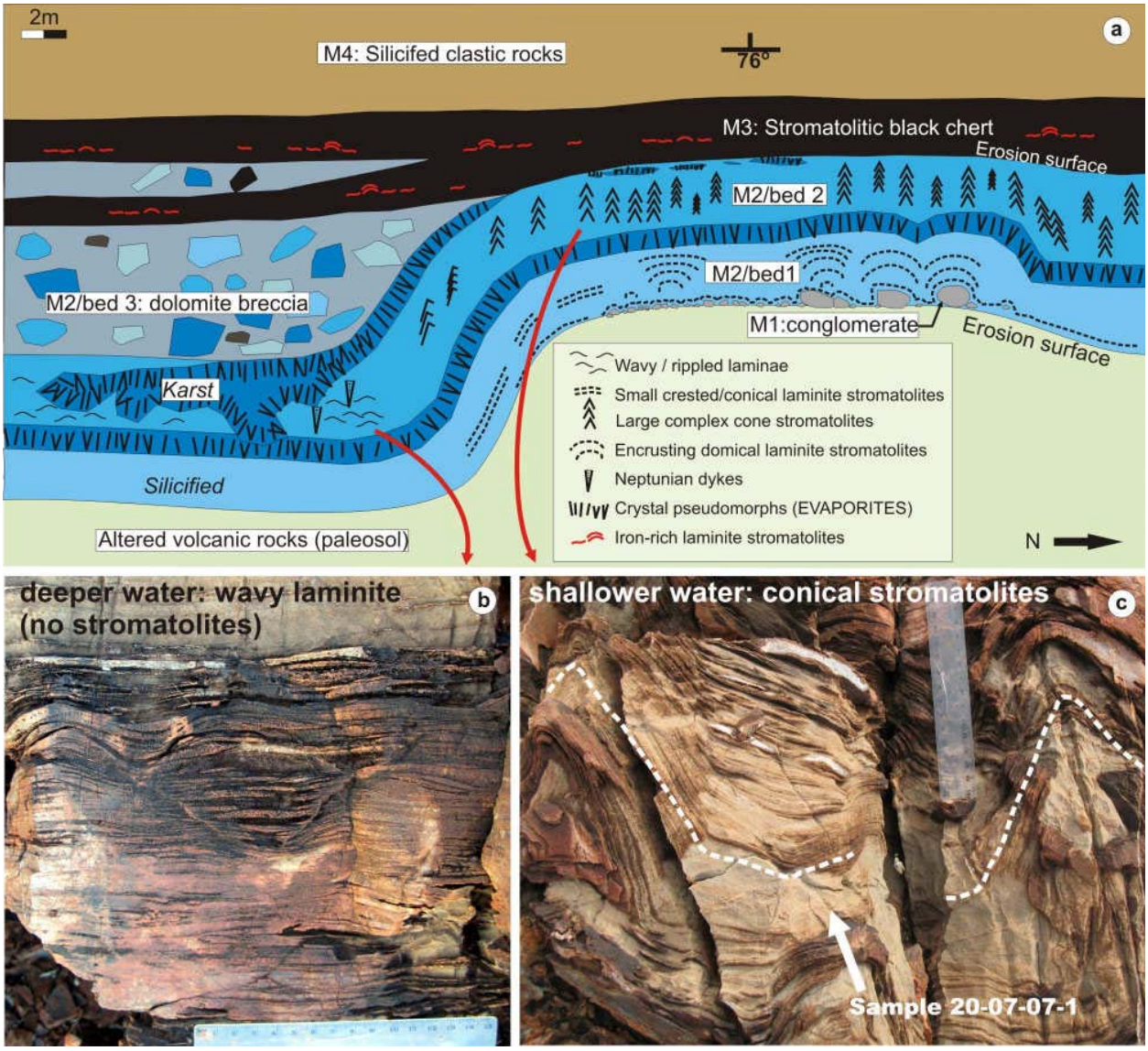
2m
a
M4: Silicifed clastic rocks
76°
M3: Stromatolitic black chert
Erosion surface
M2/bed 2
M2/bed1
M2/bed 3: dolomite breccia
M1:conglomerate
Erosion surface
Karst
Silicified
Altered volcanic rocks (paleosol)
Wavy / rippled laminae
Small crested/conical laminite stromatolites
Large complex cone stromatolites
Encrusting domical laminite stromatolites
Neptunian dykes
Crystal pseudomorphs (EVAPORITES)
Iron-rich laminite stromatolites
N
deeper water: wavy laminite
(no stromatolites)
b
shallower water: conical stromatolites
c
Sample 20-07-07-1

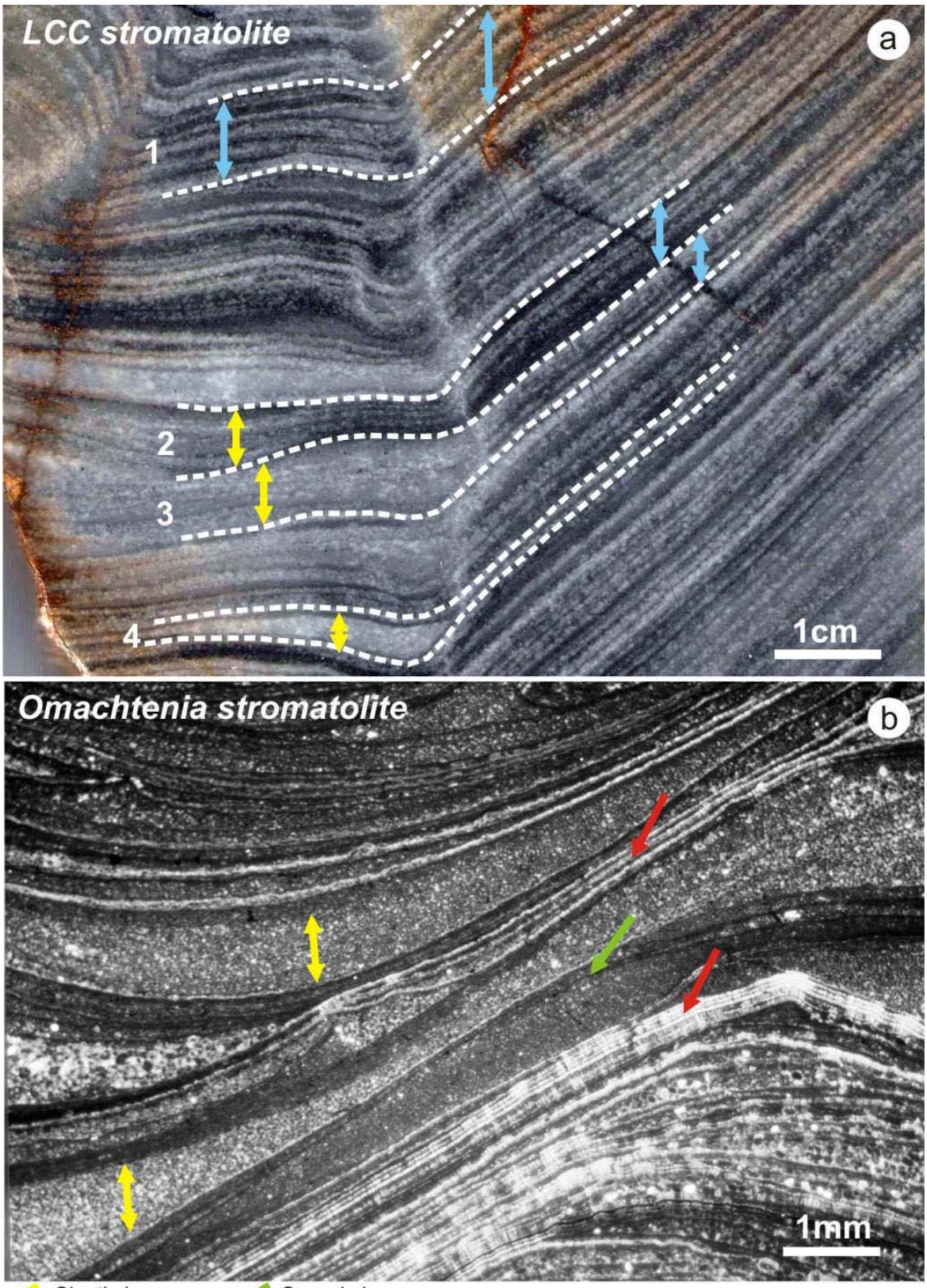
LCC stromatolite
a
1
2
3
4
1cm
Omachtenia stromatolite
b
1mm
Clastic layers
Organic layers
Layers formed by crystal precipitation organic film
Layers formed by adhesion of particles - or crystal precipitation on - organic film

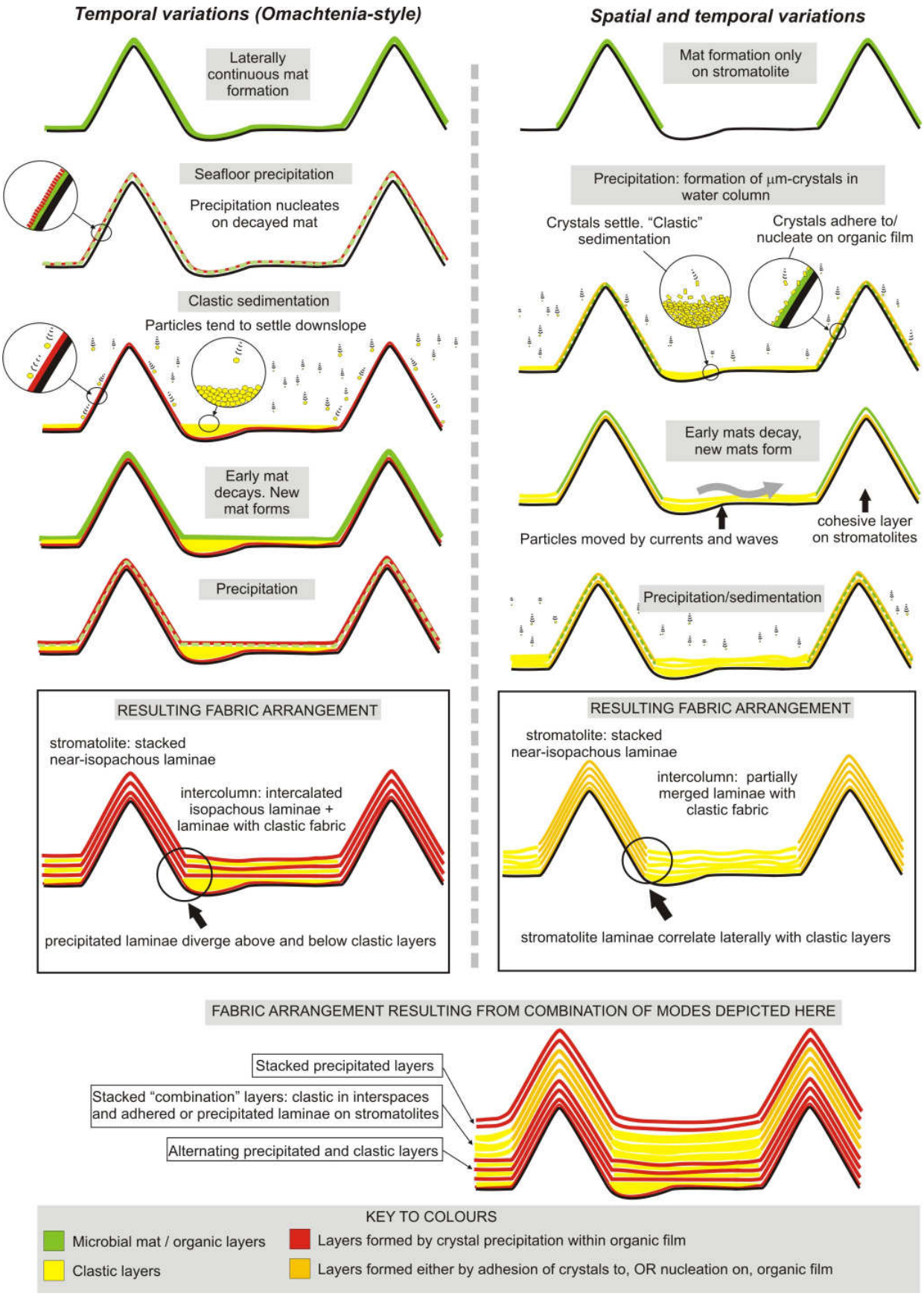
Temporal variations (Omachtenia-style)
Laterally continuous mat formation
Seafloor precipitation
Precipitation nucleates on decayed mat
Clastic sedimentation
Particles tend to settle downslope
Early mat decays. New mat forms
Precipitation
RESULTING FABRIC ARRANGEMENT
stromatolite: stacked near-isopachous laminae
intercolumn: intercalated isopachous laminae + laminae with clastic fabric
precipitated laminae diverge above and below clastic layers
Spatial and temporal variations
Mat formation only on stromatolite
Precipitation: formation of μm-crystals in water column
Crystals settle. "Clastic" sedimentation
Crystals adhere to/ nucleate on organic film
Early mats decay, new mats form
Particles moved by currents and waves
cohesive layer on stromatolites
Precipitation/sedimentation
RESULTING FABRIC ARRANGEMENT
stromatolite: stacked near-isopachous laminae
intercolumn: partially merged laminae with clastic fabric
stromatolite laminae correlate laterally with clastic layers
FABRIC ARRANGEMENT RESULTING FROM COMBINATION OF MODES DEPICTED HERE
Stacked precipitated layers
Stacked "combination" layers: clastic in interspaces and adhered or precipitated laminae on stromatolites
Alternating precipitated and clastic layers
KEY TO COLOURS
Microbial mat / organic layers
Clastic layers
Layers formed by crystal precipitation within organic film
Layers formed either by adhesion of crystals to, OR nucleation on, organic film

Supplementary Figure 1: Geological map of the study area (a) and regional map (b) showing location of study area (b modified from [17])

Supplementary Figure 2: Evolving morphology of encrusting/domical stromatolite through bed 1 at Anchor Ridge. (a) Outcrop photo of encrusting/domical stromatolite. Numbered increments on scale rule = 10cm. (b) Sketch map of the outcrop in (a), showing geometry of laminae. Dotted lines represent cm-high palisade (crystal) layers. Uppermost strata shown consist of large, acicular crystal pseudomorphs. Locations of images in Figures 1, 2 and S3 are indicated.

Supplementary Figure 3: Fabrics in middle to upper strata of encrusting/domical stromatolites studied at "Anchor Ridge". (a) Outcrop showing horizontal lamination overprinted by large crystal pseudomorphs that grew in the subsurface. (b) Polished slab showing acicular crystal pseudomorphs. The slight radiating habit of the crystals leads to a lanceolate (thin, elongate leaf-shape) appearance of crystals in this face, which was cut perpendicular to bedding. (c) Polished slab showing side of an encrusting/domical stromatolite at the level where precipitated fabrics (arrow) become abundant. (d) polished slab showing basal section of acicular crystal pseudomorphs. (e) Polished slab showing detail of precipitated fabric on side of an encrusting/domical stromatolite. (f) Polished slab showing detail of precipitated layer on the paleohorizontal surface of an encrusting/domical stromatolite. Scale bar in all images is approximately 1cm.

Supplementary Figure 4: Dolomite microfabrics in thin section view, plane polarized light. (a) D1 dolomite. (b) D2 and D3 (euhedral) dolomite with chert. (c) D2 dolomite around larger dolomite crystals. (d) D2 dolomite at the margin of D1 dolomite crystals. Plane polarized light.

Supplementary Figure 5: Representative Raman spectrum of organic-rich lamina in encrusting/domical stromatolite, showing quartz, dolomite, and disordered carbonaceous material (G and D bands in the carbon first order region).

Supplementary Figure 6: Cuspate swale stromatolite fabrics in outcrop and polished slab. (a) Cross section view of stromatolite in outcrop. Frame is approximately 40cm wide. (b) Intercolumn space with low angle cross lamination (outcrop, cross section view). Ruler at base is 15cm long. (c) Left hand margin showing transition from stromatolite fabric to interspace fabric. (d) Polished slab showing fabric at the stromatolite's apex. (e) Scan of a polished slab showing transition of fabrics at stromatolite margin: stromatolite apex to the left.

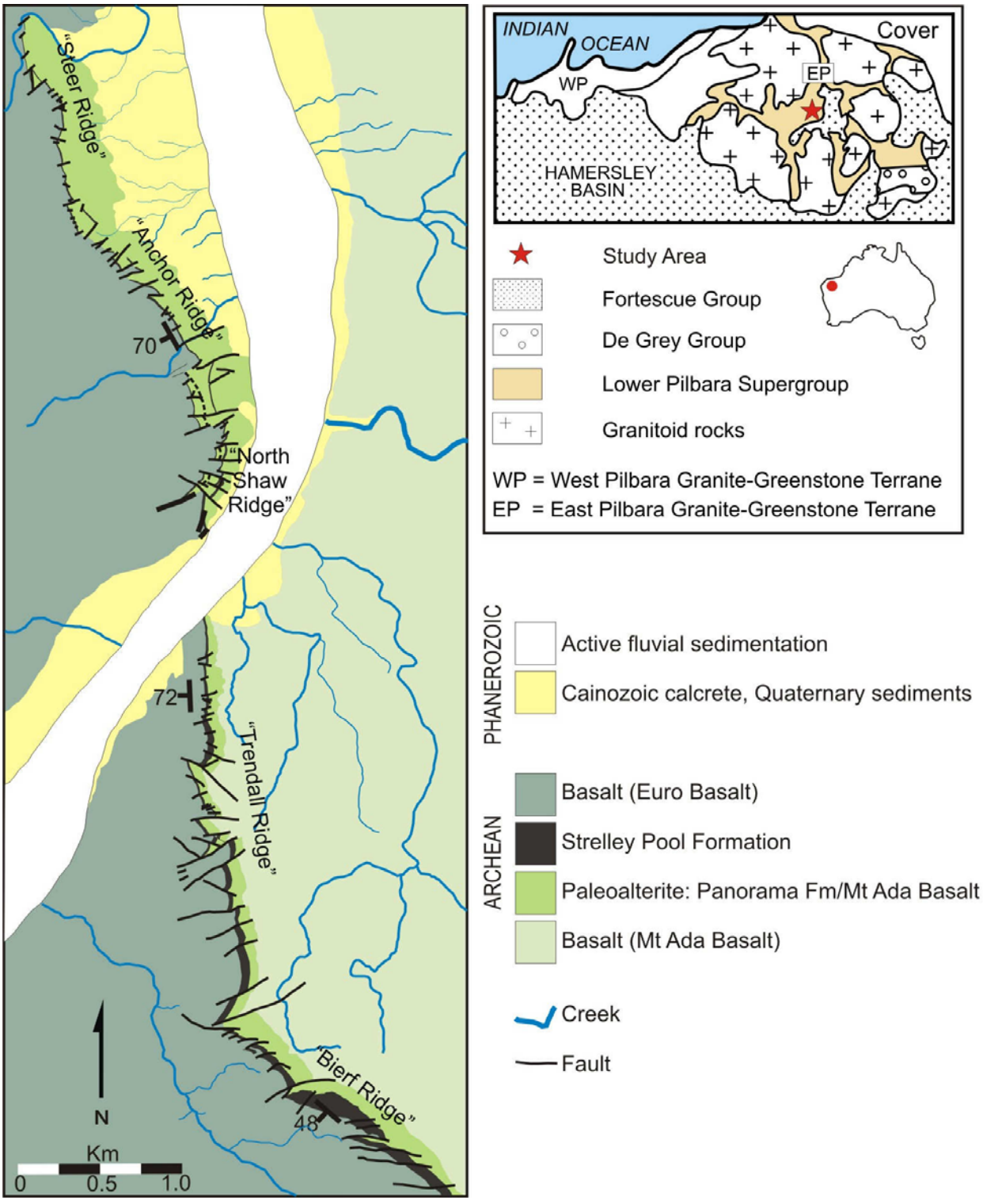
"Steer Ridge"
"Anchor Ridge"
70
"North Shaw Ridge"
72
"Trendall Ridge"
"Bierf Ridge"
48
N
Km
0
0.5
1.0
INDIAN
OCEAN
Cover
WP
EP
HAMERSLEY BASIN
Study Area
Fortescue Group
De Grey Group
Lower Pilbara Supergroup
Granitoid rocks
WP = West Pilbara Granite-Greenstone Terrane
EP = East Pilbara Granite-Greenstone Terrane
PHANEROZOIC
Active fluvial sedimentation
Cainozoic calcrete, Quaternary sediments
ARCHEAN
Basalt (Euro Basalt)
Strelley Pool Formation
Paleoalterite: Panorama Fm/Mt Ada Basalt
Basalt (Mt Ada Basalt)
Creek
Fault

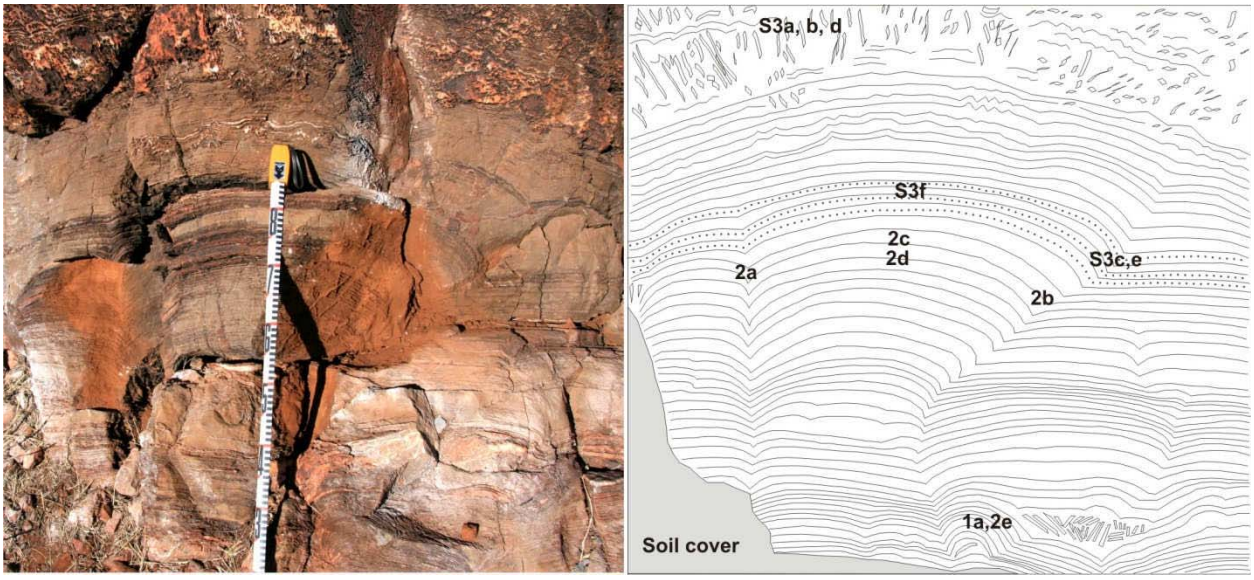
S3a, b, d
S3f
2c
2d
S3c,e
2a
2b
1a,2e
Soil cover

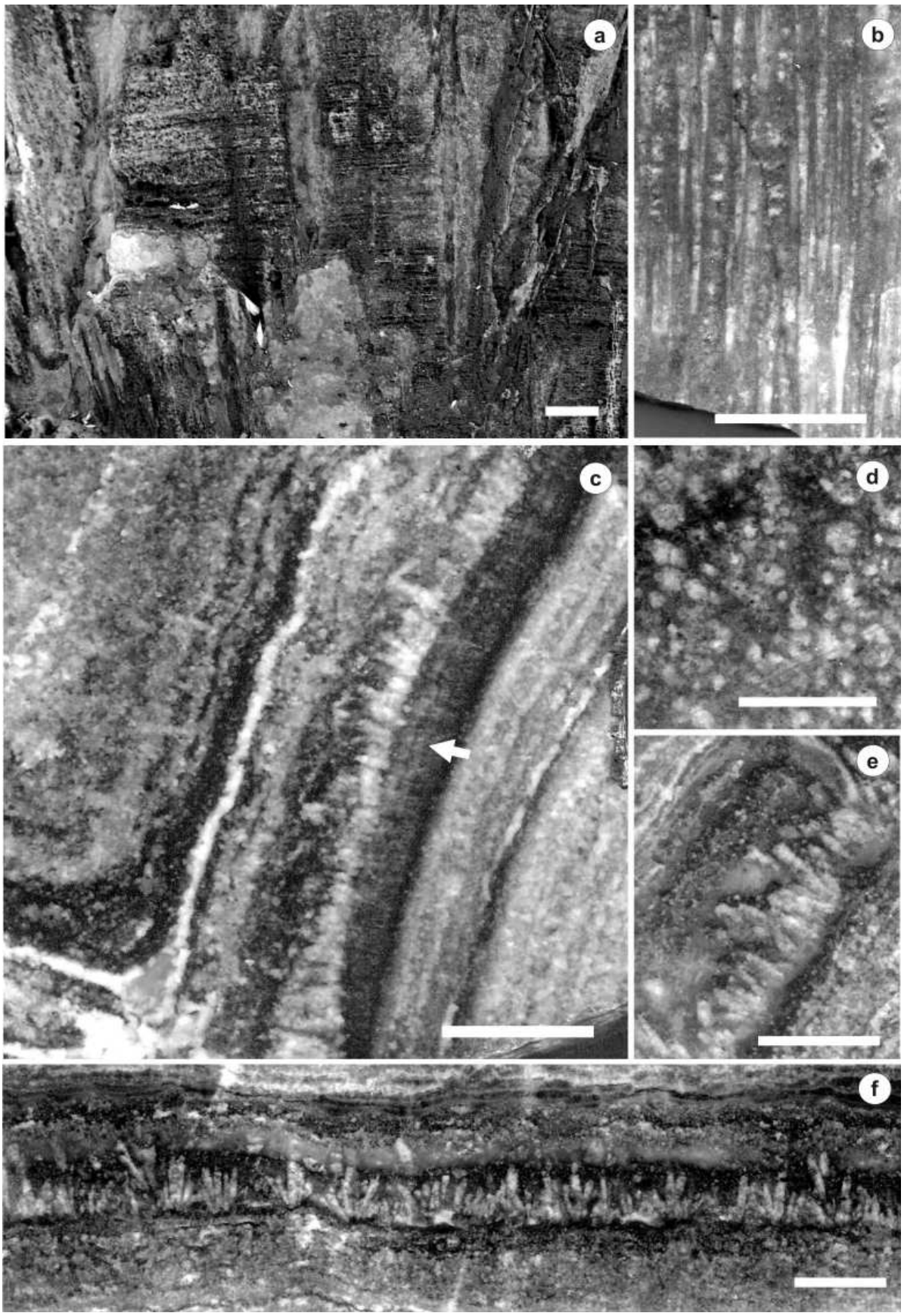
a
b
c
d
e
f

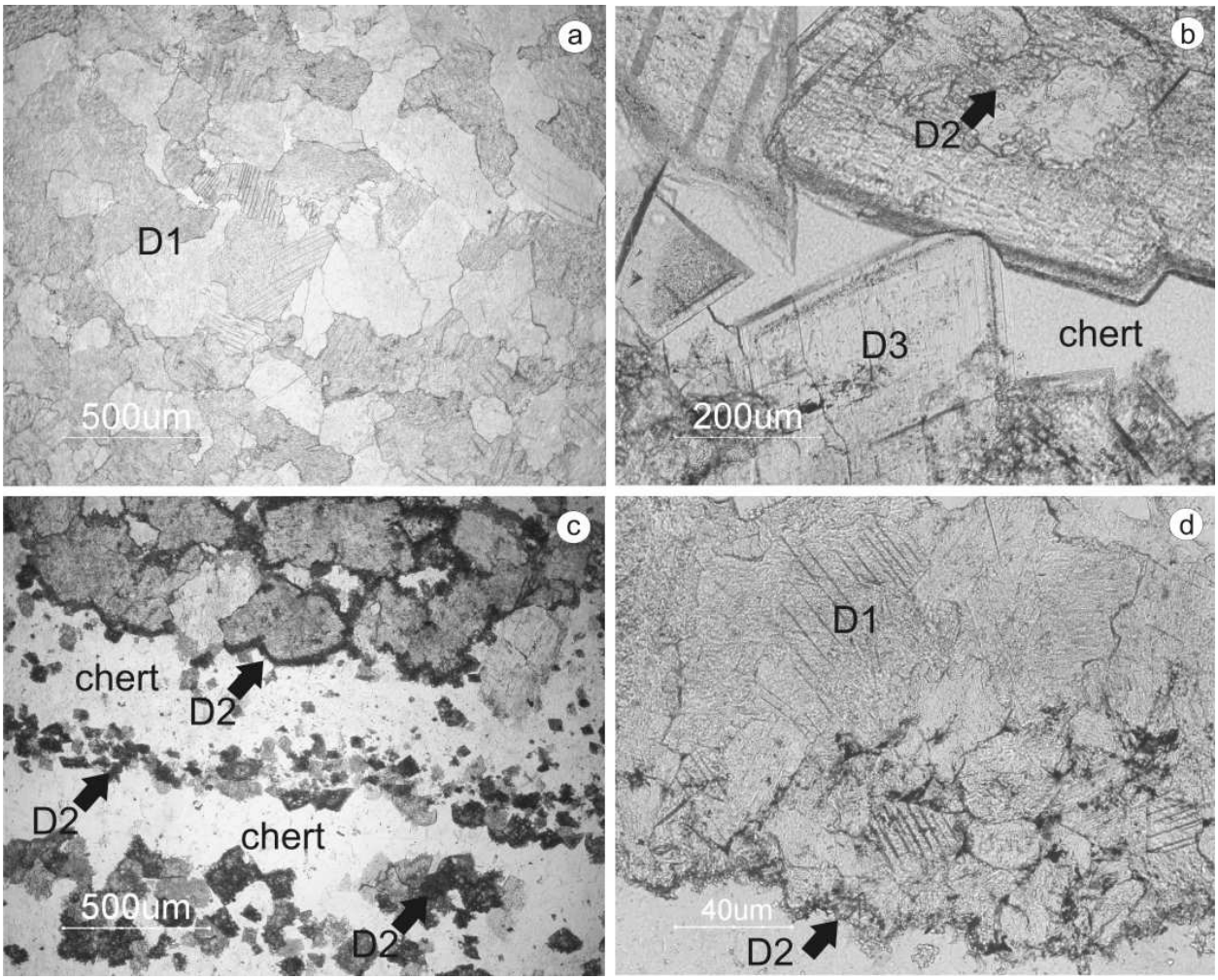
a
D1
500um
b
D2
D3
chert
200um
c
chert
D2
D2
chert
500um
D2
d
D1
40um
D2

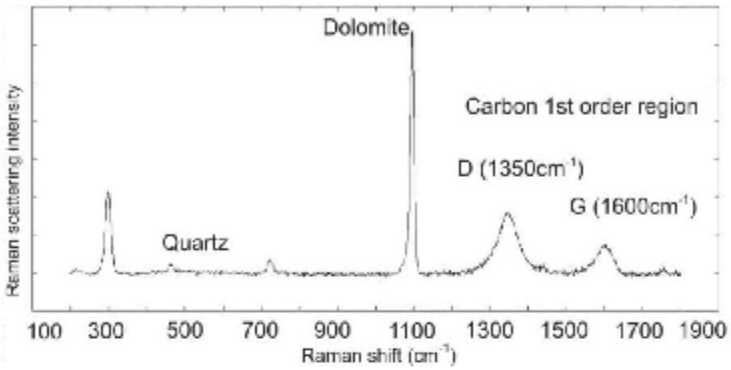
Dolomite
Carbon 1st order region
D (1350cm-1)
G (1600cm-1)
Quartz
Raman scattering intensity
100 300 500 700 900 1100 1300 1500 1700 1900
Raman shift (cm-1)

Figure S5

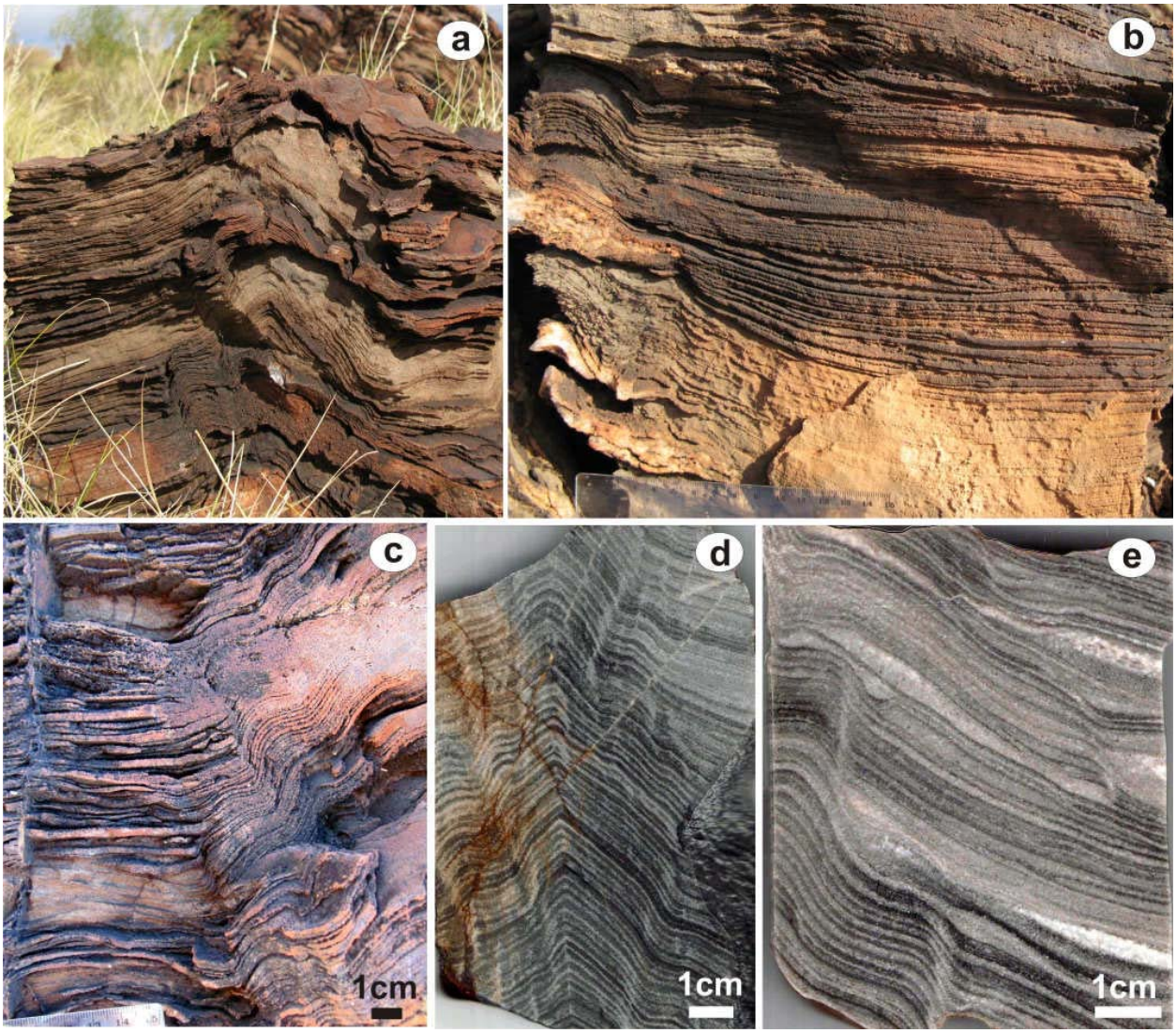
a
b
c
1cm
d
1cm
e
1cm